JOURNAL OF IRON AND STEEL RESEARCH, INTERNATIONAL. 2015, 22(9): 804-811

Precipitation and Growth of Inclusions in Solidification Process of Steel

Ying XU[1], Yao-guang WU[2], Cai-jun ZHANG[3], Li-guang ZHU[3]
(1. College of Materials Science and Engineering, Hebei Province Key Laboratory of Inorganic Nonmetallic Materials, North China University of Science and Technology, Tangshan 063009, Hebei, China; 2. Shijiazhuang Iron & Steel Co., Ltd., Hebei Iron & Steel Group, Shijiazhuang 050031, Hebei, China; 3. College of Metallurgy and Energy, North China University of Science and Technology, Tangshan 063009, Hebei, China)

Abstract: The formation and growth behavior of inclusions in the liquid steel were studied based on 45 steel by virtue of high temperature confocal laser scanning microscope. The structures of all kinds of complex inclusions formed in the process of cooling and solidification of liquid steel were analyzed, and disregistries between various inclusions were calculated. The results showed that inclusions with high melting point precipitated firstly, and inclusions with low disregistries precipitated later. The latter precipitated and grew up on the surface of the former, and finally clear layered complex inclusions formed. The low disregistry mechanism could not fully explain the forming reasons of all complex inclusions, but no matter which kind of mechanism leading to the formation of complex inclusions, its basic principle is that the first precipitated phase provides a low nuclear power interface for the latter, which can reduce the nucleation interface and strain energy barrier of the latter.

Key words: collision; growth; complex inclusion; disregistry

Non-metallic inclusions in molten steel could cause internal and surface quality defects of steel, which has a negative effect on tensile resistance, fatigue resistance and wear resistance of steel. Metallurgical workers was plagued on how to control, reduce and remove the non-metallic inclusions in steel, especially on the development of clean steel and special steel[1]. All of these put forward higher requirements on the control of non-metallic inclusions in steel. Generally, the precipitation of high melting point non-metallic inclusions with large number and small size occurred in the early time of solidification process of liquid steel. During different periods of the whole steelmaking, such as the steelmaking, refining and continuous casting processes, the type, quantity, size and property of inclusions are always changing. At the same time, the single inclusion precipitated in the early time may further change into complex inclusions with different properties. In the free cutting steel, for example, oxide inclusions with high melting point and high hardness, which were formed in the deoxidation alloying process, will change to complex inclusions with low melting point and low hardness by coating with sulfide in the solidification process of molten steel. At the same time, the harmful oxide inclusions change into beneficial complex inclusions finally. In addition, in order to improve the microstructures and properties of steel, the emergence of oxide metallurgy technology has become reasonable controlling methods of inclusions in steel. Therefore, the behavior and formation mechanism of inclusions in the molten steel during different periods is essential to better ontrol the non-metallic inclusions in steel.

In recent decades, metallurgical workers[1,2] did a lot of researches on the growth, floatation and removal of the inclusions in steel. The studies showed that inclusions precipitated through several chemical reactions, then nucleated under suitable condition, and finally grew up and floated out. The main factors of collision growth of inclusions in molten steel were the concentration of inclusion particles and the wettability between inclusions and liq-

Foundation Item: Item Sponsored by Natural Science Foundation of Hebei Province of China (E2013209207)
Biography: Ying XU, Doctor, Professor; **E-mail**: yuyingdddd@sina.cn; **Received Date**: April 10, 2014
Corresponding Author: Yao-guang WU, Master, Engineer; **E-mail**: wuyaoguang1983@sina.com

uid steel. The growth of inclusions was mainly based on diffusion, collision and polymerization[2]. Some scholars[3-8] also studied the collision growth and floatation of inclusions by numerical simulation and water simulation in different flow fields, and observed the regularity of collision growth and floatation of inclusions[9]. Yao and Zhang[10] investigated the rules of collision and growth of inclusions in molten steel by confocal laser scanning microscope (CLSM). The formation of complex inclusions in the solidification of molten steel has been reported by several investigators[11-15]. They concluded that inclusions were mainly precipitated in a complex layer structure, which were formed by the external inclusions growing up around the core. In conclusion, the regularity of collision growth, floatation and removal of inclusions and formation process of inclusions have been investigated. However, the studies above could not be able to further interpret the formation mechanism of complex inclusions with microscopic theory.

In this paper, the behaviors, especially the precipitation, diffusion and growth of the inclusions in liquid steel were observed by CLSM in hot test. The formation mechanism of complex inclusions in the heterogeneous nucleation was calculated and analyzed by the low disregistry theory, and the characteristic of complex inclusions was investigated, which provided a theoretical basis for the further utilization or removal of complex inclusions in steel.

1 Experimental

The formation process and mechanism of complex inclusions in 45 steel were investigated by CLSM and scanning electron microscopy with energy dispersive spectrometer (SEM-EDS). CLSM has a higher resolution and can also build an inert gas protection atmosphere at high temperature. In the metallurgical experiments, CLSM can be used to observe the behavior of inclusions in the molten steel real-timely and the phase change during the solidification process in situ, and the precise control of cold insulation can also be achieved. In the present study, the characteristics of CLSM, which can real-timely observe the behavior of inclusions and accurately control the cooling of inclusions, were mainly used.

After grinding and polishing, the samples were processed into a size of ϕ7 mm×3 mm, and put into CLSM, heated to 1 600 ℃ and held for a period of time; then, the behavior of inclusions in molten steel was observed. Then the samples were cooled to room temperature slowly; thus, there was sufficient time for the precipitation and growth of inclusions. The structures of complex inclusions were analyzed by SEM-EDS.

2 Formation of Complex Inclusions

2.1 Collision and growth

The inclusions in molten steel are always in motion, and they are prone to collide with each other and aggregate into larger complex inclusions particles, which easily float out finally.

As shown in Figs. 1(a)—1(e), small inclusion particles on the surface of the liquid steel constantly collided with inclusions around themselves, and then grew up gradually, and the schematic of collision growth is shown in Fig. 1(f). It was found that there was direct relationship between collision growth of inclusions and the distribution of the inclusions. The more densely the inclusions were distributed, the bigger the probability of collision was. At the same time, a lot of inclusions with various sizes were continually participated during floating out. Therefore, the collision growth of the inclusions not only occurred on the surface of the molten steel, but also in the floatation process. Thus, it should leave a certain time for the growth, floatation and removal of the inclusions after deoxidation alloying of molten steel process.

The inclusions formed during collision growth were analyzed by EDS, and the results showed that the main compositions were Ti-Mg-Al-Ca-S-O complex inclusions, as well as a small amount of MnS, which precipitated with high melting point Ti_2O_3 and Al_2O_3 inclusions. Thermodynamic calculation indicated that MnS would precipitate during solidification, and should not present in the molten steel[16]. What's more, the high melting point inclusions in liquid steel, which were wrapped by the low melting point inclusions, became easy to float out and remove. The current calcium treatment process was also based on this theory.

However, in order to improve the structure of steel by the oxide metallurgy technology, the collision growth may easily make the inclusions grow, float and remove, which can induce the nucleation of intragranular ferrite. Therefore, the long time stabilization of liquid steel may be detrimental for the oxide metallurgy technology.

2.2 Diffusion growth

The inclusions in liquid steel began to nucleate

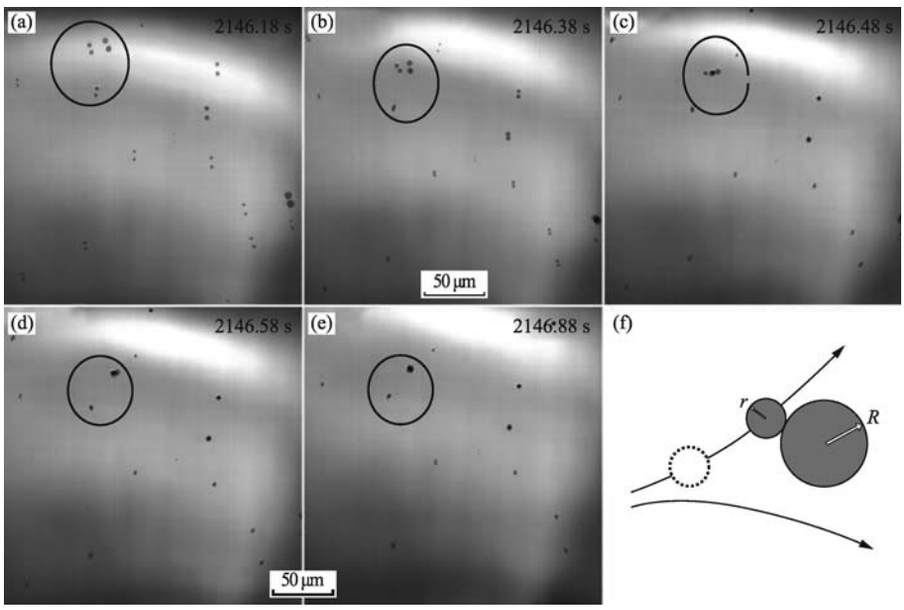

Fig. 1 In-situ observation images at 1559.7 ℃ (a-e) and schematic of the inclusions formed by collision growth (f)

from deoxidation alloying, and precipitated and grew through elements diffusion and chemical reaction. The schematic of diffusion growth was shown in Fig. 2. In present study, the complex inclusions with larger particle size and clear structure were obtained by slowly cooling to extend the diffusion growth of inclusions.

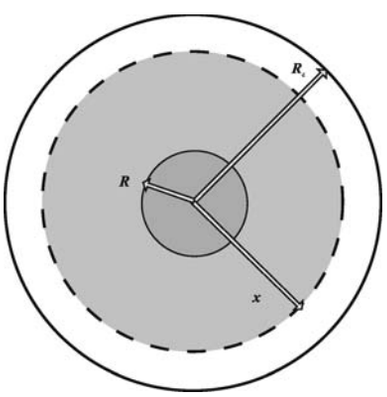

Fig. 2 The diffusion-growth schematic of inclusions

The samples obtained by slowly cooling, grinding, polishing and etching process were observed by SEM-EDS. According to the precipitation temperature obtained by the thermodynamic calculation[16], the complex inclusions could be divided into three categories: high melting point complex inclusions (precipitated at 1 600 ℃, class I, Fig. 3(a)), high melting complex inclusions attached with lower melting inclusions (precipitated at 1 400 ℃, class II, Figs. 3(b) and3(c)), low melting complex inclusions (precipitated at 1 000 ℃, class III, Figs. 3(d) and 3(e)).

3 Formation Mechanism of Inclusions

3.1 Disregistry analysis of the inclusions

Disregistry can accurately characterize the lattice matching between various types of materials. Nowadays, two-dimensional disregistry is mainly used for calculation. Low disregistry mechanism shows that the lower the disregistry between different crystalline materials is, the better the coherent relationship is. In the precipitation and growth process of inclusions, the precipitation is effective and preferential when the first precipitated materials provide a low-energy interface and reduce the $(hkl)_s$ interfacial energy and the stress energy barrier. To some extent, the two-dimensional disregistry calculated results can be used to explain the causes of complex inclusions.

The definition of two-dimensional disregistry (or plane disregistry), proposed by Bramfitt[17], is expressed by Eq. (1):

$$\delta_{(hkl)_n}^{(hkl)_s}=\sum_{i=1}^{3}\frac{|(d_{[uvw]_s^i}\cos\theta)-d_{[uvw]_n^i}|}{d_{[uvw]_n^i}/3}\times 100\% \qquad (1)$$

where, $(hkl)_s$ is the low index crystal plane of substrate phase; $[uvw]_s$ is the low index direction of $(hkl)_s$ crystal plane; $(hkl)_n$ is the low index crystal plane of crystalline phase; $[uvw]_n$ is the low index direction of $(hkl)_n$ crystal plane; $d_{[uvw]_s}$ is the atomic spacing of $[uvw]_s$, $d_{[uvw]_n}$ is the atomic spacing of $[uvw]_n$; θ is the angle between $[uvw]_s$ and $[uvw]_n$; and δ is the disregistry between $(hkl)_s$ and $(hkl)_n$.

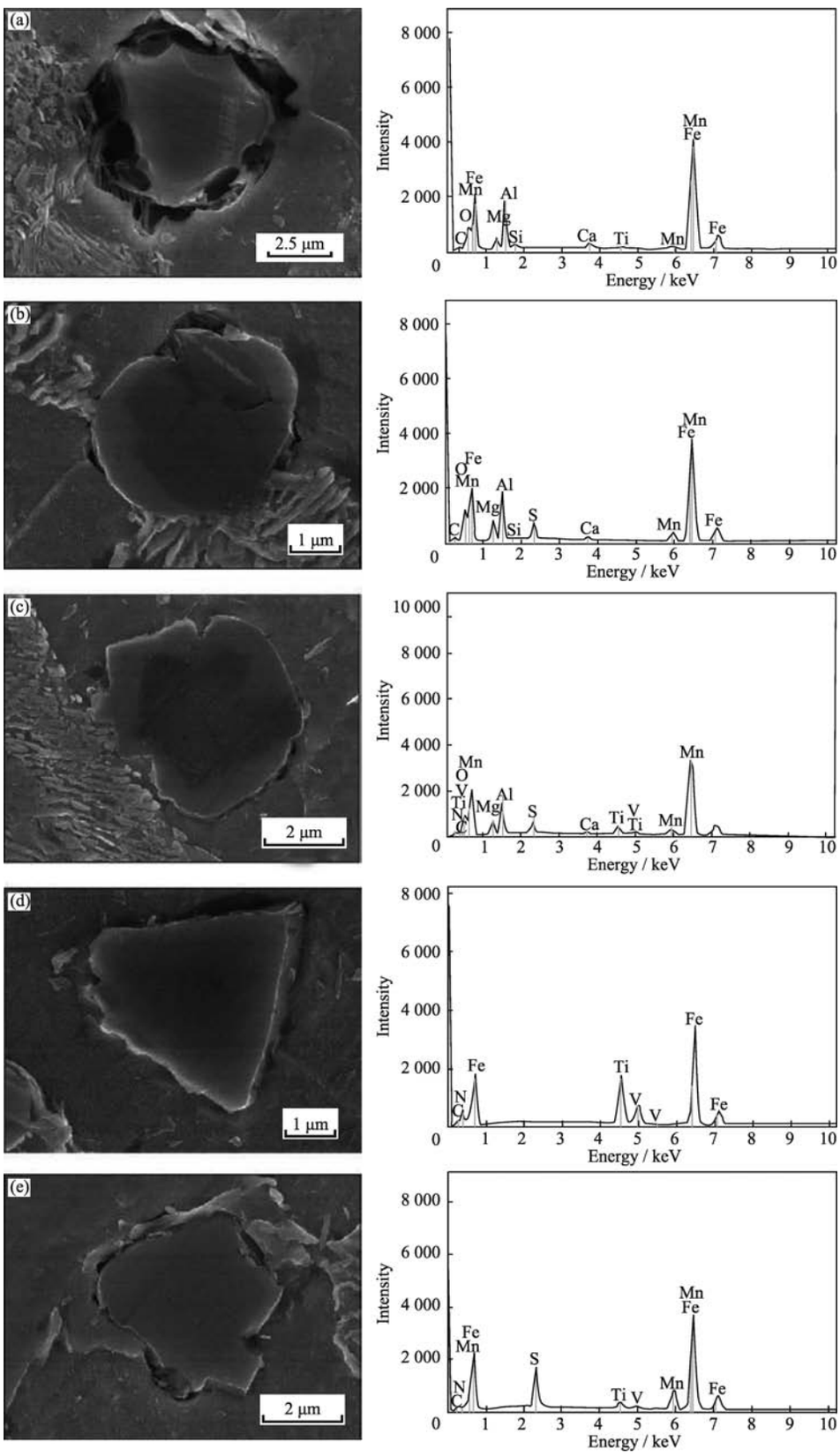

(a) Mg-Al-Ti-Ca-Si-O (class I); (b) Mg-Al-Ca-Mn-O-S (class II); (c) Mg-Al-Ti-Ca-Mn-V-C-S-O-N (class II); (d) Ti-V-C-N (class III); (e) Ti-Mn-V-C-S-N (class III).

Fig. 3 SEM images and EDS patterns of complex inclusions

Ref. [18] pointed out that nucleation was the most effective when δ was smaller than 6%. When δ was between 6% and 12%, the nucleation was medium effective. When δ was bigger than 12%, the nucleation was invalid. Based on the theory mentioned above, disregistries between the major inclusions were calculated during the precipitated temperature range of 45 steel. The calculated results are shown in Table 1.

As shown in Table 1, the major inclusions with the moderately effective nucleation in 45 steel were Ti_2O_3 and Al_2O_3; Al_2O_3, CaO, CaS and MgS; MnO and CaO; CaO, CaS and MnS; VN, VC and MnO. The major inclusions with the most effective nucleation were Ti_2O_3, Al_2O_3 and CaO; MgS and Ti_2O_3; Ti_2O_3, MgO and MnO; Ti_2O_3, MgS and MnS; MgO, MnO and TiN; VN, VC and MgO, TiN; VN and VC.

Combining with the formation and precipitation time of the main inclusions and the low disregistry calculated results, it is found that the first precipitated high melting inclusions (e. g., Al_2O_3, Ti_2O_3) could become the cores of the following precipitated inclusions with lower disregistries (e. g., MnO, MnS, TiN). The last precipitated inclusions (e. g., VN, VC) attached to the inclusions which precipitated earlier, and the disregistries between them were very low.

Table 1 Disregistries between the major inclusions %

Base phase	Al_2O_3	Ti_2O_3	CaO	CaS	MgO	MgS	MnO	MnS	TiN	VN	VC
Al_2O_3	—	—	—	—	—	—	—	—	—	—	—
Ti_2O_3	5.91	—	—	—	—	—	—	—	—	—	—
CaO	1.76	4.41	—	—	—	—	—	—	—	—	—
CaS	17.08	11.88	16.00	—	—	—	—	—	—	—	—
MgO	11.99	13.03	13.89	16.08	—	—	—	—	—	—	—
MgS	9.32	3.63	7.70	9.36	19.03	—	—	—	—	—	—
MnO	5.95	12.60	7.84	13.42	5.40	13.40	—	—	—	—	—
MnS	10.12	4.47	8.51	8.40	19.84	0.88	15.16	—	—	—	—
TiN	12.02	13.02	13.97	16.07	0.04	12.27	5.66	12.22	—	—	—
VN	13.71	12.47	13.40	17.28	2.41	12.95	8.20	13.28	2.65	—	—
VC	13.89	12.67	13.62	16.73	1.28	12.44	6.99	12.73	1.64	0.94	—

3.2 Structure analysis of complex inclusions

The elements and structures of class I composition inclusions in Fig. 3(a) were analyzed by EDS, as shown in Fig. 4. The results indicated that the complex inclusions had clear hierarchy, from inside to outside, and the interior was wrapped by the following different elements. The melting point of the inclusions consisting of the following elements has a tendency to reduce.

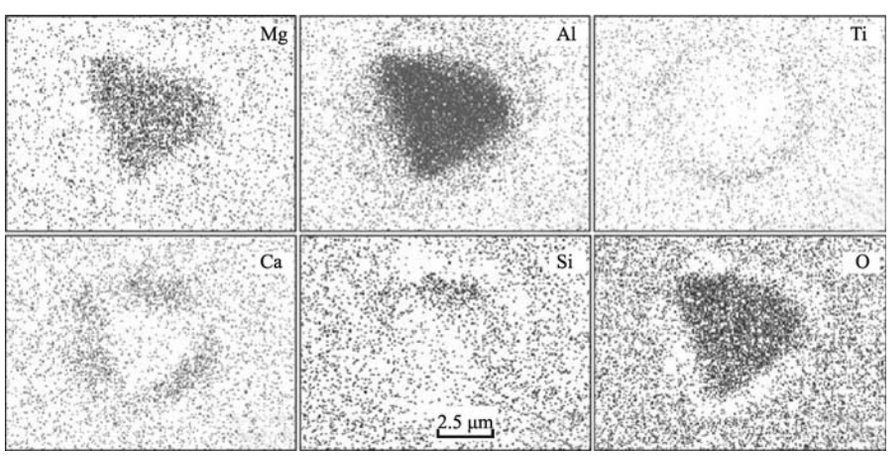

Fig. 4 EDS mapping analysis of the class I complex inclusions shown in Fig. 3(a)

As seen in Fig. 4, it could be concluded that MgO and Al_2O_3 complex inclusions with a relatively high melting point precipitated earlier (above 1 600 ℃). Then CaO, Ti_2O_3 centered on MgO, Al_2O_3 inclusions precipitated, forming multi-element complex inclusions. This phenomenon was consistent with the results in Table 1, in which there were lower disregistries among CaO, Ti_2O_3 and Al_2O_3. However, from the perspective of low disregistry, it does not have the mutual attachment and precipitation conditions between Al_2O_3 and MgO. Why this appearance occurred may be related to the nucleation energy in the precipitation process. The nucleation energy of homogeneous nucleation was much smaller than heterogeneous nucleation. Therefore, the existence of high melting inclusions provided lower interface for the later precipitated inclusions, which provided conditions for heterogeneous nucleation and reduced the nucleation energy that required to overcome during nucleation.

In the solidification process of liquid steel, TiN and MnS began to precipitate on the basis of MgO, Al_2O_3, CaO, and Ti_2O_3 deposit when the temperature reduced to about 1 400 ℃. As shown in Fig. 3(c) and Fig. 5, inclusions showed clear layered structure by successive precipitating method. Combined with the calculation results in Table 1, it is found that MnS could easily precipitate attaching on MgS, Ti_2O_3, CaS and CaO, and TiN could easily precipitate attaching to MgO and MnO because of the low disregistries between them. Meanwhile, VN and VC could precipitate attaching on TiN, but not on MnS, which was also identified by the low disregistry theory.

The structure of TiN-VN-VC inclusions was clearly shown in Fig. 6, and the carbonitride of vanadium precipitated attaching on TiN. When the temperature decreased to about 1 000 ℃, VN began to precipitate. The calculation results showed that the disregistries between VN and MgO, TiN, MnO were small. While MgO had precipitated earlier and been wrapped by the first precipitation inclusions, VN easily precipitated attaching on TiN and MnO.

VC began to precipitate when the temperature decreased to 900 ℃. The disregistries between VC and VN, TiN, MnO were very small. Therefore, VC precipitated easily attaching on VN, TiN and MnO, and then complex inclusions were formed finally.

By comparing the structure of several complex inclusions and calculated results, it can be found that low disregistry theory could not fully explain the formation mechanism of all the complex inclusions. For example, MgO and Al_2O_3 shown in Figs. 4 and 5 precipitated attaching on each other, but they did not meet the requirement of low disregistry theory. In addition, it was found that lots of MnS and TiN complex inclusions precipitated attaching to each other, as shown in Fig. 7. However, no matter which kind of inclusions between MnS and TiN precipitated as base phase, the disregistries

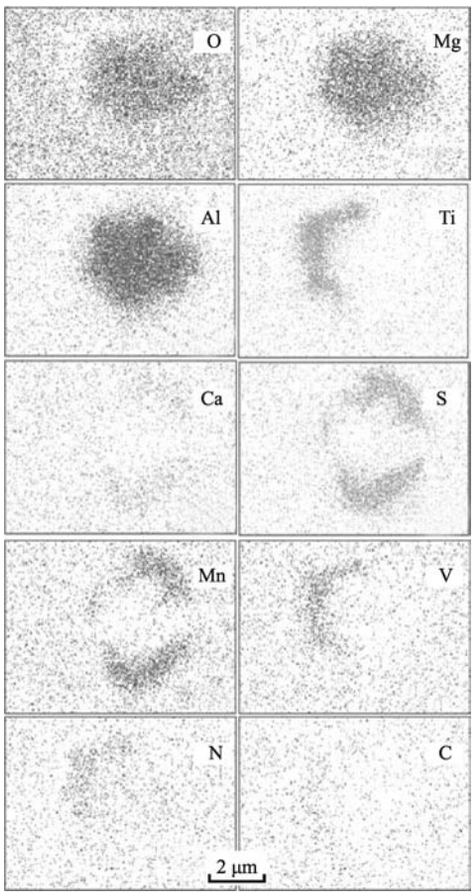

Fig. 5 EDS mapping analysis of the class II complex inclusions shown in Fig. 3(c)

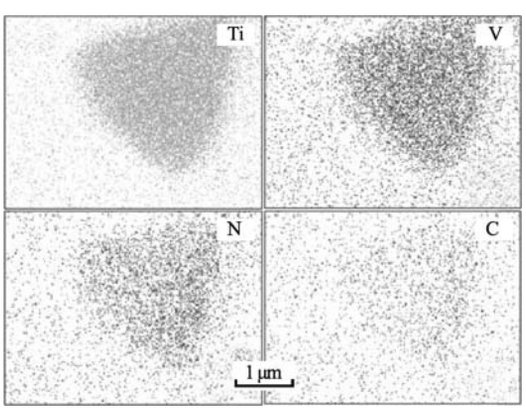

Fig. 6 EDS mapping analysis of the class III complex inclusions shown in Fig. 3(d)

between them were larger than the effective nucleation value, which could not be explained by low disregistry theory. Therefore, the formation mechanism of MnS-TiN complex inclusions should be analyzed for further study. However, whatever the mechanism leads to the formation of the complex inclusions, its basic principle is that the first precipitated phase provides a low energy interface for the latter to reduce the interfacial energy and stress energy barrier of nucleation.

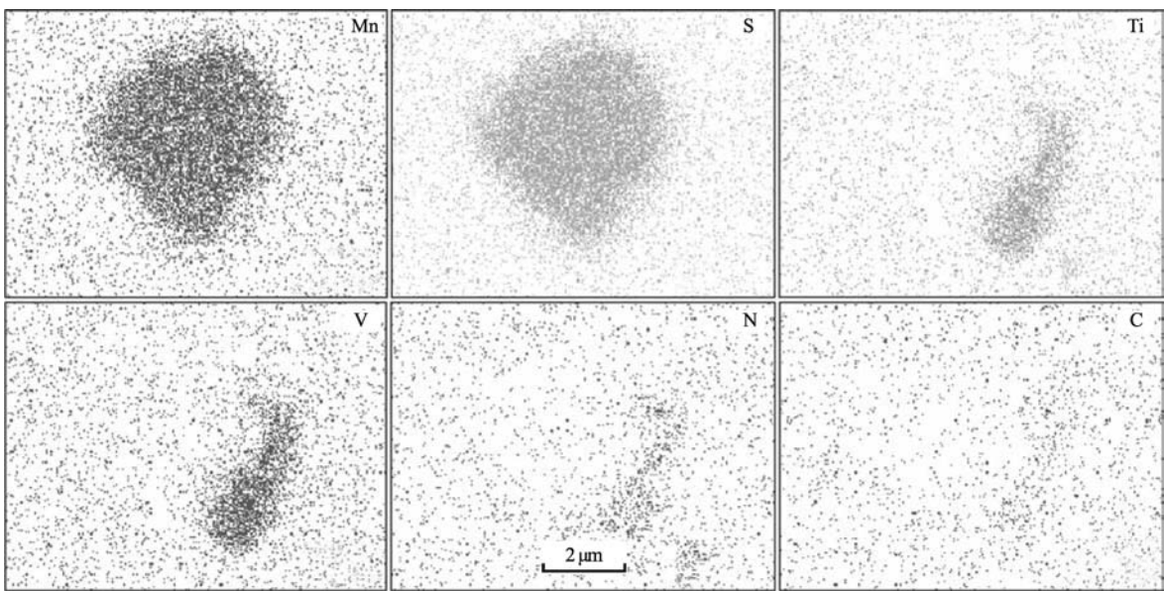

Fig. 7 EDS mapping analysis of the class III complex inclusions shown in Fig. 3(e)

The following conclusions were obtained by calculating the two-dimensional disregistries between non-metallic inclusions and acicular ferrite. The order of non-metallic inclusions that were most beneficial to the precipitation of acicular ferrite was: VN, VC, TiO, MgO, TiN, TiC, NbN, NbC and MnO. Among them, the minimum disregistries between acicular ferrite and VN, VC were 1.8% and 2.7%, respectively, which were very conducive for intracrystalline ferrite to nucleation on their surface. Therefore, if alloying elements were reasonably introduced into the liquid steel, complex inclusions would continually form as well as the above analysis with the decrease of the temperature of molten steel. The outermost layer of complex inclusions would be crucial to induce the precipitation of acicular ferrite.

4 Conclusions

(1) Inclusions in molten steel remain the state of motion, unceasingly floating to the surface, and collision growth occurred in the floatation process and on the surface.

(2) Complex inclusions can be roughly divided into high melting complex inclusions, complex inclusions with lower melting inclusions attaching, and low melting complex inclusions. All of these were formed in different periods.

(3) The formation process of some complex inclusions could be explained by low disregistry theory.

For example, the formation process of Mg-Al-Ti-Ca-Mn-V-C-S-O-N complex inclusions was that CaO and Ti_2O_3 precipitated attaching on the high melting MgO and Al_2O_3 complex inclusions with decreasing temperature, MnS and TiN precipitated attaching on MgS, Ti_2O_3, CaS, CaO, MgO and MnO, VN deposited on TiN and MnO, and VC finally precipitated attaching on VN, TiN and MnO.

(4) Low disregistry theory could not fully explain the formation cause of all complex inclusions. No matter what kind of mechanism led to the complex inclusion formation, the basic principle was that the first precipitated phase providing a low energy interface to reduce the latter one's interfacial energy and stress energy barrier of nucleation.

(5) By the analysis of the structure of inclusions and their formation mechanism in 45 steel, the number and size of harmful high melting inclusions could be reduced and controlled by changing the following conditions, such as controlling the component content of deoxidation alloying elements, strengthening the effect of wash heat and argon stir-

ring effect, and selecting rational liquid steel refining process and reasonable calm time. What's more, the number and size of harmful low melting inclusions could also be controlled by adjusting the cooling system during the rolling process.

References:

[1] L. G. Zhao, J. China Rare Earth Soc. 20 (2002) 202-206.
[2] B. W. Zhang, B. W. Li, Y. D. He, J. Iron Steel Res. 17 (2005) No. 6, 19-25.
[3] D. Zhang, H. Terasaki, Y. I. Komizo, Acta Mater. 58 (2010) 1369-1378.
[4] W. Yang, J. Cao, X. H. Wang, Z. R. Xu, J. Yang, J. Iron Steel Res. Int. 20 (2011) No. 9, 6-12.
[5] W. Yang, H. Duan, L. Zhang, Y. Ren, JOM 65 (2013) 1173-1180.
[6] J. Yang, X. H. Wang, M. Jiang, W. J. Wang, J. Iron Steel Res. Int. 18 (2011) No. 7, 8-14.
[7] L. G. Zhao, K. Liu, J. Iron Steel Res. 14 (2002) No. 6, 19-24.
[8] H. Lei, J. C. He, Acta Metall. Sin. 43 (2007) 1195-1200.
[9] Q. Yue, Z. S. Zou, Q. F. Hou, J. Iron Steel Res. Int. 17 (2010) No. 5, 6-10.
[10] R. F. Yao, C. J. Zhang, Henan Metallrugy 18 (2010) No. 2, 7-8.
[11] S. F. Yang, J. S. Li, L. F. Zhang, K. Peaslee, Z. F. Zhang, J. Iron Steel Res. Int. 17 (2010) No. 7, 1-6.
[12] Y. N. Wang, Y. P. Bao, M. Wang, L. C. Zhang, Y. N. Chen, Metall. Mater. Trans. B 44 (2013) 1144-1154.
[13] Z. H. Jiang, S. J. Li, Y. Li, J. Iron Steel Res. Int. 18 (2011) No. 2, 14-17.
[14] D. Y. Wang, M. Liu, C. J. Liu, M. F. Jiang, Journal of Northeastern University 34 (2013) 373-377.
[15] Y. Ren, Y. Wang, S. Li, L. Zhang, X. Zuo, S. N. Lekakh, K. Peaslee, Metall. Mater. Trans. B 45 (2014) 1291-1303.
[16] L. G. Zhu, Y. G. Wu, Y. H. Han, Steelmaking 29 (2013) 53-56.
[17] N. Pang, B. Song, Q. J. Zhai, B. Wen, J. Univ. Sci. Technol. Beijing 32 (2010) 179-190.
[18] R. C. Cochrane, J. Mater. Sci. 17 (1982) 732-740.